NANO LETTERS

2007
Vol. 7, No. 9
2660−2665

Novel Bioinorganic Nanostructures Based on Mesolamellar Intercalation or Single-Molecule Wrapping of DNA Using Organoclay Building Blocks

Avinash J. Patil, Mei Li, Erik Dujardin, and Stephen Mann*

Centre for Organized Matter Chemistry, School of Chemistry, University of Bristol, Bristol BS8 1TS, United Kingdom

Received May 4, 2007; Revised Manuscript Received July 2, 2007

ABSTRACT

Nanosheets or nanoclusters of aminopropyl-functionalized magnesium phyllosilicate (AMP) were prepared in water by exfoliation and used as structural building blocks for the preparation of DNA-based hybrid nanostructures in the form of ordered mesolamellar nanocomposites or highly elongated nanowires, respectively. The former consisted of alternating layers of single sheets of AMP interspaced with intercalated monolayers of intact double-stranded DNA molecules of relatively short length (~700 base pairs) that were accessible to small molecules such as ethidium bromide. In contrast, the nanowires comprised isolated micrometer-long molecules of λ-DNA or plasmid DNA that were sheathed in an ultrathin organoclay layer and which were either protected from or remained accessible to endonuclease-mediated clipping depending on the extent of biomolecule wrapping. Both types of hybrid nanostructures showed a marked increase in the DNA melting (denaturation) temperature, indicating significant thermal stabilization of the confined biomolecules. Our results suggest that nanoscale building blocks derived from organically modified inorganic clays could be useful agents for enhancing the chemical, thermal, and mechanical stability of isolated molecules or ensembles of DNA. Such constructs should have increased potential as functional components in bionanotechnology and nonviral gene transfection.

Previous reports on the fabrication of functional nanohybrid materials for nanoelectronics and bionanotechnology emphasize the importance of controlling several key factors such as nanoparticle synthesis and stabilization, surface modification and interparticle recognition, assembly and disassembly of 2-D and 3-D superstructures, and the design and integration of multiple components across several length scales.[1,2] In many cases, biomolecules have been used as building blocks in nano-, meso-, and macroscopic architectures,[3,4] and deoxyribonucleic acid (DNA) in particular has proved to be an attractive and promising candidate for the design and assembly of functional nanostructural scaffolds and as a template for the directed growth of metallic or polymeric nanoparticles and nanowires.[5−11] Other studies have placed great emphasis on the development of DNA-based nanostructures in association with polycationic lipids, biopolymers, or polypeptides as nonviral vectors for cellular delivery and transfection.[12−16]

Recently, inorganic materials in the form of layered structures have been used to prepare bioinorganic nanocomposites that could have applications in controlled storage/release, sensing, and DNA delivery.[17−20] In this regard, advances in materials synthesis to produce mesolamellar structures with covalently linked organic moieties has enabled a wide range of organoclay nanocomposites to be prepared with enhanced functionality.[21] Significantly, protonation of interlayer aminopropyl groups in certain synthetic magnesium phyllo(organo)silicates produces exfoliated (delaminated) organoclay dispersions that can be subsequently reassembled in the presence of various negatively charged drug molecules[22] or biomolecules such as myoglobin, hemoglobin, or glucose oxidase[23] to produce intercalated hybrid nanocomposites with ordered mesolamellar structure and biofunctionality. Moreover, the exfoliated dispersions can be fractionated by gel chromatography to produce organoclay polycationic clusters of approximate composition, $[(CH_2)_3NH_2]_4Si_4Mg_3O_8(OH)_2$, that can be used as building blocks to isolate single molecules of various proteins and enzymes.[24]

In this paper, we develop and extend the above methods for the fabrication of new types of DNA-based nanostructures. Specifically, we demonstrate two protocols that illustrate the use of aminopropyl-functionalized magnesium phyllosilicate (AMP, unit cell composition $[(CH_2)_3NH_2]_8Si_8Mg_6O_{16}(OH)_4$) as a source of structural building blocks for the electrostatically induced capture and storage of DNA

* Corresponding author. E-mail: s.mann@bris.ac.uk.

10.1021/nl071052q CCC: $37.00
Published on Web 08/17/2007

Scheme 1. Preparation of DNA/Organoclay Nanostructures.

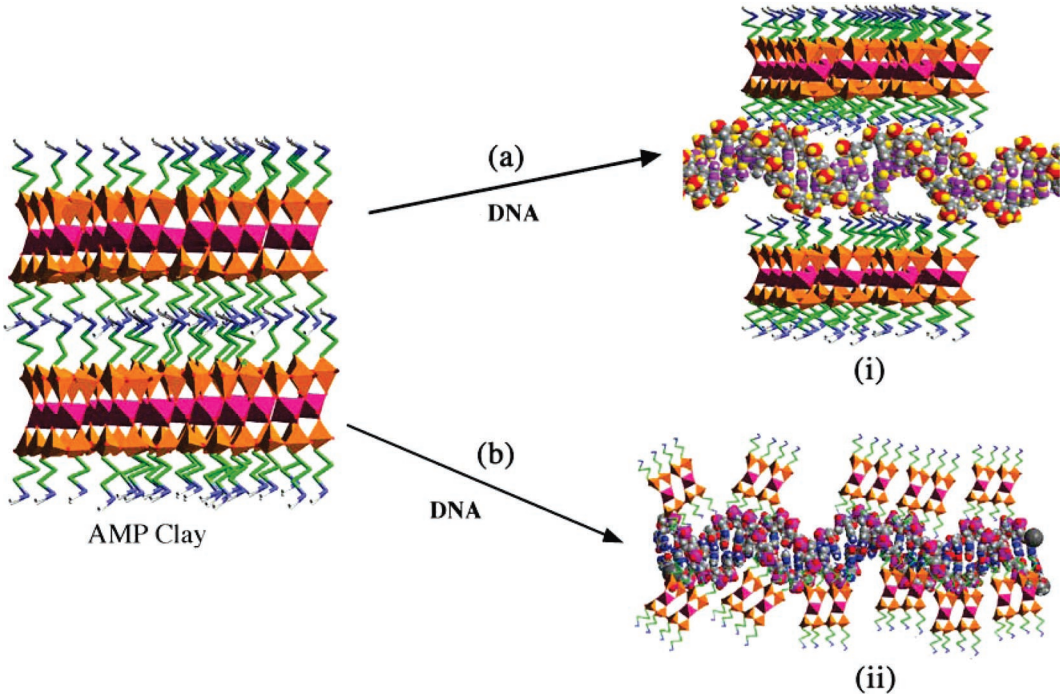

(a) Protonation of aminopropyl side chains of as-synthesized AMP clay in water results in exfoliation and formation of dispersed nanosheets. Addition of stoichiometric quantities of DNA gives rise to electrostatically induced reassembly of the organoclay layers in association with biomolecule intercalation to produce an ordered mesolamellar nanocomposite. (b) Exfoliation and fractionation by gel chromatography results in organoclay polycationic clusters that bind and condense to produce an ultrathin organoclay sheath on individual DNA molecules, leading to molecular-scale isolation of the double-helical strands.

in the form of intercalative mesolamellar assemblies or wrapped single molecules (Scheme 1). The positively charged organoclay building blocks were produced by water-induced exfoliation of AMP into ultrathin sheetlike nanoparticles,[23] or by gel chromatographic fractionation of the exfoliated AMP dispersion into relatively low molecular weight organoclay polycationic clusters of molecular mass, 400−700,[24] and subsequently added to DNA solutions to produce DNA/organoclay layered nanocomposites or nanowires, respectively. The hybrid nanostructures consisted respectively of ensembles or isolated molecules of intact double-stranded DNA, both of which exhibited enhanced stabilization to thermally induced denaturation. In addition, by varying the extent of organoclay binding/condensation on the surface of λ-DNA molecules, hybrid constructs that were either protected from or accessible to restriction enzyme-mediated scission could be readily prepared.

DNA/organoclay layered nanocomposites were prepared by dropwise addition of 1 mL of a solution of herring testis DNA (2.2×10^{-3} mM, 400−1000 base pairs (mean bp = 700, approximate length ~230 nm);[25] D-6898, Sigma) in Tris-HCl buffer (10 mM, pH = 8, 1 mM EDTA) to an exfoliated AMP clay dispersion (2 mL; prepared by dispersing 20 mg of the dry as-synthesized organoclay in 2 mL of distilled water followed by ultrasonication for 15 min), which consisted of sheetlike nanoparticles, ~2 nm in thickness. The DNA/organoclay precipitate was equilibrated for 24 h at room temperature and then isolated by centrifugation, followed by drying at room temperature in air. Samples analyzed by FTIR spectroscopy showed characteristic absorbances for both DNA (P−O, 1232 cm^{-1} (970 and 1090 cm^{-1} vibrations masked by organoclay peaks), and AMP (Si−C (1050 cm^{-1}), Si−O−Si (1008 cm^{-1}), Mg−O−Si (551 cm^{-1}), NH_2^+(2103 cm^{-1}), NH (1646 cm^{-1}), CH_2 (2935 cm^{-1})). Typically, 1.95×10^{-9} moles of DNA were associated with 20 mg of the organoclay matrix (UV−vis spectroscopy, $\lambda = 260$ nm), which was equivalent to a DNA entrapment efficiency of ~88% assuming negligible adsorption of the biomolecules on the external surfaces of the particles.

Intercalation of DNA molecules in the layered galleries of reassembled AMP was confirmed using powder X-ray diffraction (PXRD), which showed an expanded basal spacing (d_{001}) of 3.6 nm compared with a value of 1.6 nm for the parent organoclay (Figure 1a). The 2 nm increase in basal spacing was commensurate with intercalation of a monolayer of intact double-stranded DNA molecules aligned parallel to the plane of the aminopropyl-functionalized inorganic framework. PXRD patterns also showed retention of the typically highly disordered in-plane organoclay reflections ($d_{020,\ 110}$, $d_{130,\ 300}$), as well as the characteristic phyllosilicate peak at $2\theta = 59°$ ($d_{060,330} = 0.156$ nm), indicating that DNA intercalation did not significantly disrupt the inorganic framework during co-assembly of the hybrid mesolamellar structure. This was consistent with TEM images recorded from small fragments of the hybrid nanocomposite viewed normal to the stacking direction, which

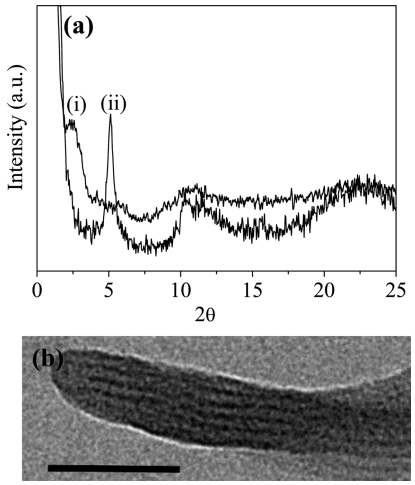

Figure 1. (a) PXRD profiles for (i) AMP/DNA nanocomposite and (ii) as-synthesized AMP clay. Large peaks in (i) and (ii) correspond to d_{001} reflections at 3.6 or 1.6 nm, respectively; the highly broadened profiles are typical of organo-functionalized magnesium phyllosilicates. (b) TEM image of AMP/DNA nanocomposite showing lattice fringes spaced a distance of 3.5 nm corresponding to an expanded mesolamellar nanocomposite (scale bar = 50 nm).

revealed periodic lattice fringes spaced at a distance of approximately 3.5 nm (Figure 1b).

Circular dichroism (CD) spectroscopy showed strong negative and positive peaks at 247 and 278 nm, respectively, (Figure 2a), which were comparable to native DNA,[26] and indicated that the double-helical structure was not significantly perturbed during intercalation of the biomolecule between the AMP layers. This was confirmed by addition of a solution of ethidium bromide to a suspension of the DNA/organoclay nanocomposite, which resulted in a shift in the optical absorbance of the dye from 480 nm (orange) to 515 nm (pink), consistent with binding of the dye specifically to the bases of the double helix (Figure 2b). Moreover, these studies indicated that the intercalated DNA molecules remained accessible to small molecules in the external solvent, presumably via diffusion through the interlayer spaces.

The effect of entrapment on the thermal stability of the biomolecules was determined by recording the melting temperature (dehybridization) profiles of free and intercalated DNA molecules at 260 nm using a UV−vis spectrophotometer attached with a Peltier temperature controller. In both cases, sigmoidal melting curves were obtained, indicating cooperative denaturation of the double helix (Figure 2c). However, the organoclay/DNA nanocomposite showed a melting temperature (T_m) of 83 °C compared with a value of 63 °C for free DNA. The significant increase in T_m by 20 °C clearly indicated a marked improvement in thermal stability of the intercalated DNA and suggested that multipoint electrostatic interactions between pendent aminopropyl groups covalently attached to the inorganic framework and counter-charged entrapped DNA molecules were responsible for the change in temperature-dependent behavior.

The above results indicate that DNA/organoclay nanocomposites with mesolamellar structure consisting of alternating layers of single sheets of aminopropyl-functionalized magnesium phyllosilicate interspaced with entrapped monolayers of intact DNA molecules can be readily prepared by electrostatically induced spontaneous co-assembly. The use of exfoliated organoclay sheets offers several advantages over conventional ion-exchange-derived intercalation approaches, which are often severely diffusion-limited and restricted to guest molecules of low molecular size and mass. Moreover, the increased thermal stability of the intercalated DNA suggests that such nanocomposites could be used for the efficient storage of ensembles of biologically active macromolecules. As the method is facile, a wide range of novel and complex layered bioinorganic nanocomposite materials should be accessible through systematic developments in the methodology.

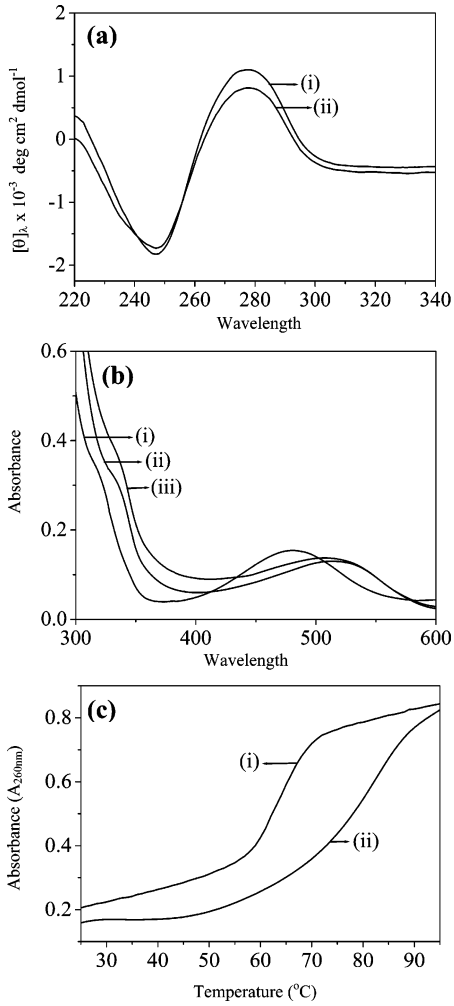

Figure 2. (a) Circular dichroism spectra for (i) native DNA (ii) organoclay-intercalated DNA, showing retention of helical structure. The small decrease in intensity at 278 nm for (ii) may be due to partial charge neutralization in the presence of the aminopropyl side chains of the organoclay. (b) UV−vis spectra of (i) ethidium bromide control solution, (ii) ethidium bromide + native DNA conjugate, and (iii) ethidium bromide + DNA/AMP clay nanocomposites showing shift of the 480 nm band to 515 nm due to binding of ethidium bromide to intercalated DNA molecules. (c) Melting curves for (i) native DNA and (ii) DNA/AMP nanocomposites showing increased thermal stability of the intercalated DNA molecules.

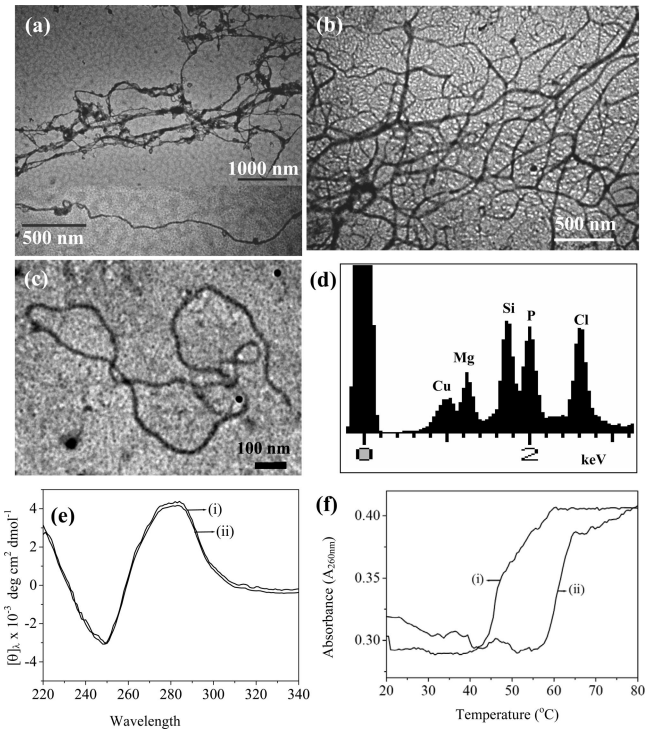

Figure 3. (a−c) Unstained TEM images showing (a) organoclay-wrapped λ-DNA nanowires (inset shows higher magnification image of a single λ-DNA molecule isolated within a continuous organoclay sheath), (b) complex network of organoclay nanowires showing fibers with thicknesses of up to 30 nm, as well as filaments with very low electron density, and (c) single organoclay-wrapped plasmid molecule. (d) EDX analysis of discrete hybrid nanostructure showing peaks for Mg/Si (organoclay) and P (DNA). (e) Circular dichroism spectra and (f) melting curves for (i) native λ-DNA and (ii) organoclay-wrapped λ-DNA.

In contrast to the above studies, single macromolecules of DNA were isolated in the form of inorganically wrapped discrete nanostructures by charge-induced encapsulation in the presence of organoclay polycationic clusters (ζ potential $= +12$ mV at pH 8). Typically, 20 μL of λ-DNA (0.05 μg/μL, New England Biolabs, UK, 48 502 base pairs, length $\sim$16 μm) solution was mixed with 20 μL of a solution of AMP polycationic clusters that were prepared by exfoliation of the as-synthesized clay in water (10 mg dry AMP/10 mL of water with ultrasonication for 5 min) followed by gel chromatography on a Sephadex G-50 column. Alternatively, 10 μL of plasmid DNA (0.04 μg/μL, pUC19 New England Biolabs, 2686 base pairs) solution was added to 2 μL of the solution of organoclay polycationic clusters. In both cases, the DNA/organoclay solutions were vortexed at room temperature for 12 h.

TEM studies of unstained samples of λ-DNA after incubation in a solution of AMP polycationic clusters revealed well-defined nanofilaments that were highly flexible and continuous over lengths of several micrometers (Figure 3a). Typically, discrete nanowires, $\sim$15 nm in width, as well as bundled and interconnected thicker nanofilaments up to $\sim$30 nm across, could be routinely imaged due to the high electron density associated with surface binding and condensation of organoclay coatings of at least 6 nm in thickness (Figure 3a,b, Supporting Information Figure S1). Filaments of lower contrast could also be observed (Figure 3b), which possibly represented individual DNA molecules with monolayer or submonolayer coverage of condensed AMP polycationic clusters. Significantly, unstained samples of native DNA could not be imaged due to the low electron density of the 2 nm wide biomolecular structure and confirmed that the contrast observed for the AMP-treated samples was associated with surface deposition of the organoclay. Similar results were obtained when plasmid DNA was mixed with solutions of the AMP polycationic clusters to produce 12−14 nm thick coiled hybrid nanostructures (Figure 3c). EDX analyses confirmed the presence of both organoclay (Si, Mg, and Cl (counterion)) and DNA (P) components in the electron dense nanowires prepared in the presence of λ-DNA or plasmid DNA (Figure 3d), and CD spectra showed in both cases characteristic peaks at 248 and 278 nm, indicating that double-stranded helical DNA structures were retained within the wrapped nanostructures (Figure 3e). Significantly, the thermal melting profiles showed sigmoidal behavior, consistent with a collective mechanism of dehybridisation, and an increase in T_m °C from 46 (native λ-DNA) to 61 °C (organoclay-wrapped λ-DNA) (Figure 3f). The enhanced thermal stability of the AMP-wrapped DNA molecules was similar to that observed for organoclay-intercalated DNA (Figure 2c), indicating that similar electrostatic interactions were present in both types of nanostructures.

AFM studies were undertaken on organoclay-wrapped single DNA molecules adsorbed onto silica substrates and imaged in air in tapping mode. Under these conditions, well-defined images of single molecules with rough surface topography and apparent heights between 2 and 10 nm were observed (Figure 4, Supporting Information Figure S2). In contrast, native (uncoated) λ-DNA showed an apparent height of 1 nm, confirming that the AMP-treated DNA molecules were associated with nanometer-thick sheaths of condensed AMP oligomers that were wrapped around the biomolecular template. As the apparent heights were less than the electron-dense nanowires commonly observed by TEM, the AFM results were predominantly associated with DNA molecules with relatively low levels of organoclay binding. Significantly, histograms of the apparent heights of the wrapped single molecules showed profiles that could be deconvoluted into three components centered at heights at 3.2, 5.4, and 7.6 nm and spaced at intervals of around 2.2 nm (Figure 4b). Assuming an apparent height of 1 nm for the DNA molecular core, these values were consistent with the successive binding and condensation of organoclay clusters to produce coatings of just over 1 nm in thickness, which would be equivalent to a single sheet of the AMP structure. Moreover, the histograms indicated that monolayer coverage was predominant over bi- and trilayer wrapping (Figure 4b), consistent with a template-directed process of organoclay nucleation that was dependent on strong primary interactions between the negatively charged DNA phosphate groups and polycationic AMP clusters.

Organoclay wrapping of λ-DNA was also confirmed by agarose gel electrophoresis. The samples were separated by horizontal gel electrophoresis on a 1.2% agarose gel in TAE

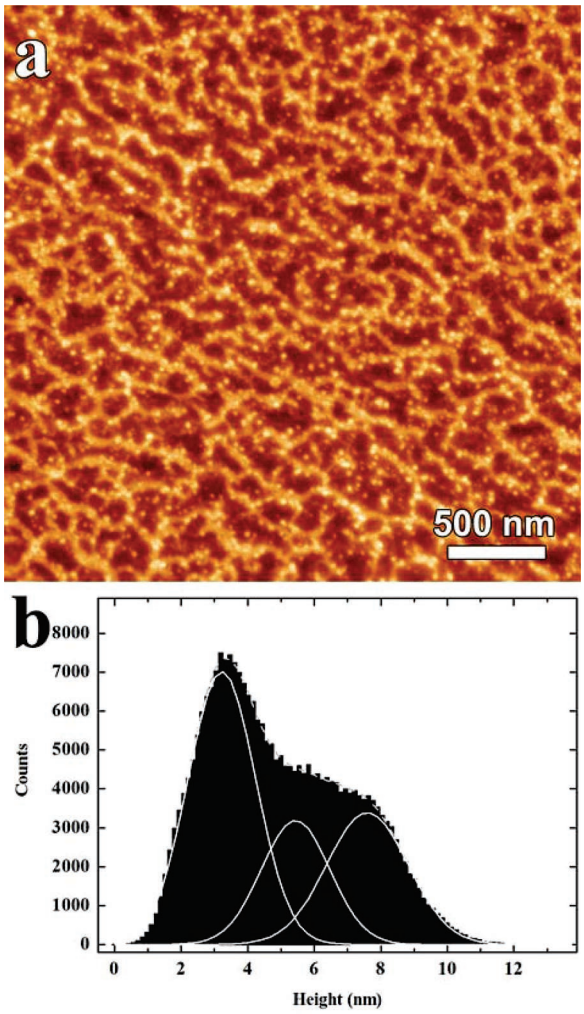

Figure 4. (a) Tapping mode AFM image of λ-DNA/AMP nanocomposite filaments deposited on a silicon wafer with a 100 nm thick oxide surface showing organoclay wrapping and surface decoration of individual biomolecules. (b) Histogram of apparent heights with associated deconvolution curves showing dominant values at 3.2, 5.4, and 7.6 nm.

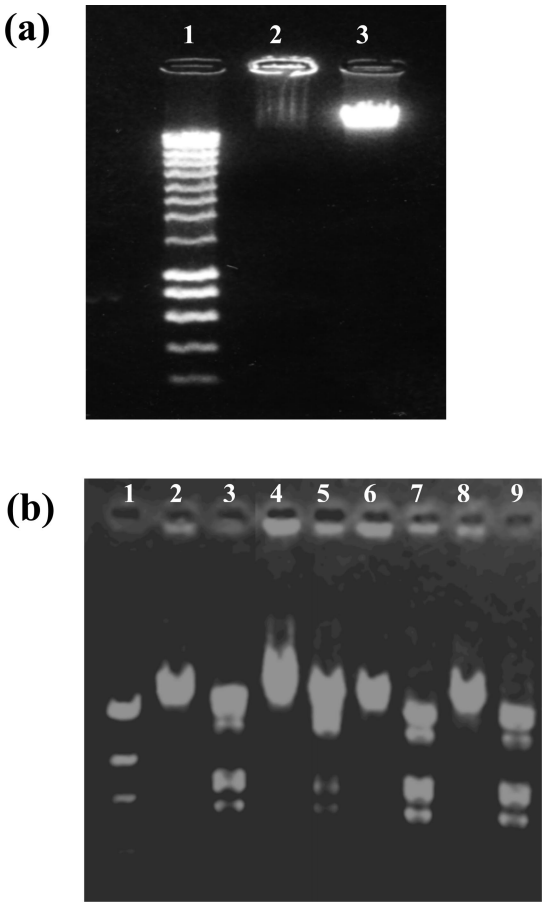

Figure 5. (a) Gel electrophoresis profiles; Lanes: (1) calibration ladder (eurodentec, 200 base-pair), (2) hybrid DNA/organoclay nanowires, and (3), native DNA. Loaded gels were stained with a solution of 0.1% ethidium bromide for 15 min and visualized in an ultraviolet transilluminator. Images were recorded using a Kodak DC40 digital camera. (b) Gel electrophoresis profiles showing electrophoretic mobility of DNA/organoclay nanowires prepared at different reactant ratios before and after treatment with the restriction enzyme, BamH1. Lanes: (1) control ladder (DNA + Hind III digest), (2) native DNA, (3) native DNA + BamH1, (4) DNA/organoclay (1:1), (5) DNA/organoclay (1:1) + BamH1, (6) DNA/organoclay (1:0.5), (7) DNA/organoclay (1:0.5) + BamH1, (8) DNA/organoclay (1:0.025), (9) DNA/organoclay (1:0.025) + BamH1.

(tris/acetate/EDTA buffer) and gels run for 1 h at 100 V. Whereas samples of free λ-DNA migrated toward the positive electrode (Figure 5a, lane 3), the λ-DNA/organoclay nanowires (Figure 5a, lane 2) were mainly retained in the holding well, indicating that the extent of binding/condensation of AMP oligomers along the helical backbone of the DNA molecules was sufficient to induce charge neutralization or reversal in the hybrid construct.

To further investigate the chemical accessibility of the entrapped λ-DNA molecules, samples were prepared at different λ-DNA/organoclay oligomer ratios and the resulting constructs combined with the restriction enzyme BamH1 to determine their susceptibility to enzymatic clipping. In each case, TEM investigations showed that the as-synthesized materials were in the form of wirelike nanostructures (data not shown). Corresponding gel electrophoresis profiles of constructs prepared at λ-DNA/organoclay v/v ratios of 1:1, 1:0.5, and 1:0.025 (Figure 5b, lanes 4, 6, and 8, respectively) showed staining both in the holding well and within the gel, suggesting that the samples consisted of a mixture of hybrid nanostructures with variable surface charge due to incomplete organoclay wrapping of the DNA molecules. Decreasing the amount of organoclay reduced the staining in the holding well and increased the extent of migration of the mobile component into the gel until it was essentially identical to the mobility observed for native λ-DNA (Figure 5b, lane 2).

The above samples were subsequently incubated at 37 °C for 2 h with the restriction enzyme BamH1 (reaction mixture: 2 μL of λ-DNA/organoclay dispersion, 1 μL of 10× restriction buffer, 1 μL of BamH1 (Sigma-Aldrich, 10 units/μL,) and 6 μL of distilled water), and the solutions then quenched by rapid cooling. Treatment with BamH1 had no influence on the electrophoretic mobility of the fully wrapped λ-DNA molecules, which remained immobilized in the holding well (Figure 5b, lanes 5, 7, and 9), indicating that the ultrathin organoclay sheath was able to protect the

DNA from endonuclease activity. In contrast, the restriction enzyme was able to access exposed GGATCC recognition sites in the partially wrapped electrophoretically mobile constructs to produce lower molecular weight fragments that migrated further into the gel (Figure 5b, lanes 5, 7, and 9). This was particularly prevalent for samples prepared at lower organoclay contents (Figure 5b, lanes 7 and 9), consistent with the presence of partially encased DNA strands that were exposed and thus susceptible to endonuclease activity.

In summary, our results indicate that magnesium (organo)-phyllosilicate nanosheets/nanoclusters are effective building blocks for DNA-entrapped hybrid nanocomposites. We highlight two simple methods for the fabrication of organoclay/DNA nanostructures either in the form of a mesolamellar nanocomposite or single-molecule wrapped nanowires. The former are produced from the spontaneous DNA-induced reassembly of exfoliated sheets of the cationic organoclay and results in the periodic intercalation of a monolayer of intact double-stranded DNA molecules between adjacent layers of the reconstituted inorganic framework. Interlayer confinement of the DNA molecules increases their thermal stability and limits accessibility to small molecules that are capable of diffusing through the gallery spaces. Alternatively, individual DNA molecules can be isolated by wrapping in an ultrathin inorganic sheath produced by electrostatic binding and condensation of organoclay polycationic clusters specifically on the biomolecular template. The encapsulated DNA molecules retain their native helical structure and anisotropy, can be protected from or remain accessible to enzymatic clipping depending on the extent of surface wrapping, and are thermally stabilized with regard to denaturation. Extension of these methods should enable a wide range of new types of functional biomaterials with enhanced stability to be prepared that might be sufficiently robust for integration into bioelectronic devices, or used extensively as effective and safe nonviral delivery systems. We are currently investigating the cytotoxicity of organoclay/DNA nanostructures and their ability to act as transfection agents in cell cultures.

Acknowledgment. We thank ERSRC for financial support. A. Mahmood is acknowledged for technical assistance in preparing AFM substrates.

Supporting Information Available: High magnification TEM image of wrapped organoclay/DNA filament and AFM imaging of organoclay-wrapped λ-DNA deposited on freshly cleaved mica. This material is available free of charge via the Internet at http://pubs.acs.org.

References

(1) Katz, E.; Willner, I. *Angew. Chem., Int. Ed.* **2004**, *43*, 6042−6108.
(2) Niemeyer, C. M. *Angew. Chem., Int. Ed.* **2001**, *40*, 4128−4158.
(3) Dujardin, E.; Mann, S. *Adv. Mater.* **2002**, *14*, 775−788.
(4) van Bommel, K. J. C.; Friggeri, A.; Shinkai, S. *Angew. Chem., Int. Ed.* **2003**, *42*, 980−999.
(5) Storhoff, J. J.; Mirkin, C. A. *Chem. Rev.* **1999**, *99*, 1849−1862.
(6) Barun, E.; Eichen, Y.; Sivan, U.; Ben-Yoseph, G. *Nature* **1998**, *391*, 775−778.
(7) Patolsky, F.; Weizmann, Y.; Lioubashevski, O.; Willner, I. *Angew. Chem., Int. Ed.* **2002**, *41*, 2323−2327.
(8) Richter, J.; Seidel, R.; Kirsch, R.; Mertig, M.; Pompe, W.; Plaschke, J., Schackert, K. *Adv. Mater.* **2000**, *12*, 507−510.
(9) Monson, C. F.; Woolley, A. T. *Nano. Lett.* **2003**, *3*, 359−363.
(10) Kinsella, J. M.; Ivanisevic, A. *J. Am. Chem. Soc*. **2005**, *127*,3276−3277.
(11) Ma, Y.; Zhang, J.; He, H. *J. Am. Chem. Soc.* **2004**, *126*, 7097−7101.
(12) Kumar, C. Biological and Pharmaceutical Nanomaterials; Wiley-VCH: New York, 2006.
(13) Kneur, C.; Sameti, M.; Haltner, E. G.; Schiestel, T.; Schirra, H.; Schmidt, H. K. *Int. J. Pharm.* **2000**, *196*, 257−261.
(14) Shen, H.; Tan, J.; Saltzman, W. M. *Nat. Mater.* **2004**, *3*, 569−574.
(15) Salem, A. K.; Searson, P. C.; Leong, K. W. *Nat. Mater.* **2003**, *2*, 668−671.
(16) Roy, I.; Ohulchanskyy, T. Y.; Bharali, D. J.; Pudavar, H. E.; Mistretta, R. A.; Kaur, N.; Prasad, P. N. *Proc. Natl. Acad. Sci. U.S.A.* **2005**, *102*, 11539−11544.
(17) Ruiz-Hitzky, E.; Darder, M.; Aranda, P. *J. Mater. Chem.* **2005**, *15*, 3650−3662.
(18) Choy, J. H.; Kwak, S. Y.; Jeong, Y. J.; Park, J. S. *Angew. Chem., Int. Ed.* **2000**, *39*, 4042−4045.
(19) Tyner, K. M.; Roberson, M. S.; Berghorn, K. A.; Li, L.; Gilmour, R. F., Jr.; Batt, C. A.; Giannelis, E. P. *J. Controlled Release* **2004**, *100*, 399−409.
(20) Desigaux, L.; Belkacem, M. B.; Richard, P.; Cellier, J.; Leone, P.; Cario, L.; Leroux, F.; Taviot-Gueho, C.; Pitard, B. *Nano Lett.* **2006**, *6*, 199−204.
(21) Burkett, S. L.; Press, A.; Mann, S. *Chem. Mater.* **1997**, *9*, 1071−1073.
(22) Holmstrom, S. C.; Patil, A. J.; Butler, M.; Mann, S. *J. Mater. Chem.* **2007**, http://dx.doi.org/10.1039/b705158a.
(23) Patil, A. J.; Muthusamy, E.; Mann, S. *J. Mater. Chem.* **2005**, *15*, 3838−3843.
(24) Patil, A. J.; Muthusamy, E.; Mann, S. *Angew. Chem., Int. Ed.* **2004**, *43*, 4928−4933.
(25) Rosa, M.; Dias, R.; Miguel, M. G.; Lindman, B. *Biomacromolecules* **2005**, *6*, 2164−2171.
(26) Schukin, D. G.; Patel, A. A.; Sukhorukov, G. B.; Lvov, Y. M. *J. Am. Chem. Soc.* **2004**, *126*, 3374−3375.

NL071052Q